Chelate Cooperativity and Spacer Length Effects on the Assembly Thermodynamics and Kinetics of Divalent Pseudorotaxanes
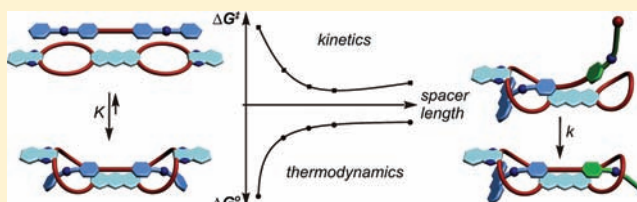
Wei Jiang,[†,§] Karol Nowosinski,[†] Nora L. Löw,[†] Egor V. Dzyuba,[†] Fabian Klautzsch,[†] Andreas Schäfer,[†] Juhani Huuskonen,[‡] Kari Rissanen,[‡] and Christoph A. Schalley*,[†]

[†]Institut für Chemie und Biochemie, Freie Universität Berlin, Takustrasse 3, 14195 Berlin, Germany
[‡]Department of Chemistry, Nanoscience Center, University of Jyväskylä, P.O. Box 35, 40014 Jyväskylä, Finland

S Supporting Information

ABSTRACT: Homo- and heterodivalent crown-ammonium pseudorotaxanes with different spacers connecting the two axle ammonium binding sites have been synthesized and characterized by NMR spectroscopy and ESI mass spectrometry. The homodivalent pseudorotaxanes are investigated with respect to the thermodynamics of divalent binding and to chelate cooperativity. The shortest spacer exhibits a chelate cooperativity much stronger than that of the longer spacers. On the basis of crystal structure, this can be explained by a noninnocent spacer, which contributes to the binding strength in addition to the two binding sites. Already very subtle changes in the spacer length, i.e., the introduction of an additional methylene group, cause substantial changes in the magnitude of cooperative binding as expressed in the large differences in effective molarity. With a similar series of heterodivalent pseudorotaxanes, the spacer effects on the barrier for the intramolecular threading step has been examined with the result that the shortest spacer causes a strained transition structure and thus the second binding event occurs slower than that of the longer spacers. The activation enthalpies and entropies show clear trends. While the longer spacers reduce the enthalpic strain that is present in the transition state for the shortest member of the series, the longer spacers become entropically slightly more unfavorable because of conformational fixation of the spacer chain during the second binding event. These results clearly show the noninnocent spacers to complicate the analysis of multivalent binding. An approximate description which considers the binding sites to be connected just by a flexible chain turns out to be more a rough approximation than a good model. The second conclusion from the results presented here is that multivalency is expressed in both the thermodynamics and the kinetics in different ways. A spacer optimized for strong binding is suboptimal for fast pseudorotaxane formation.

■ INTRODUCTION

Multivalency describes molecular recognition phenomena between the two binding partners involving multiple binding sites separated by spacers. This is widely observed in biochemistry.[1] Quite significant interaction energy increases have been found for example for pentavalent Shiga-like toxins when compared to the monovalent one.[2] Also, multivalent carbohydrate interactions have been examined quite extensively.[3] In a seminal paper on the activation of cGMP-gated membrane channels in vertebrate photoreceptors and olfactory neurons, Kramer and Karpen[4] reported an up to 1000-fold activity increase of polymer-linked cGMP dimers over monovalent ones. A clear-cut correlation of spacer length with channel activation was observed: Too short spacers bind in a monovalent fashion and have effects comparable to those of cGMP. With spacers able to bridge the distance between binding sites and causing some strain, the effect increases until the optimal binding situation is realized. Longer spacers suffer from additional entropic penalties for conformational restrictions and lose some of their potency with increasing length. Diestler and Knapp[5] simulated these binding events with statistical mechanics calculations whose trends compare well with these experimental data. Similar trends

were also observed in a study of intramolecular binding of covalently linked ligands to human carbonic anhydrase.[6] This study arrives at the conclusion that flexible spacers longer than the optimal distance between the binding sites will still be effective, though not optimal.

The multivalency concept has been transferred to synthetic supramolecules and was utilized for the construction of more complex architecture from suitably programmed building blocks.[7] Besides binding energy increases, multivalency also contributes to controlling the geometry of the complex through multipoint attachment between host and guest. It therefore represents an important concept in supramolecular synthesis besides templation,[8] self-assembly,[9] and self-sorting.[10] For example, multivalent calixarene[11] and cyclodextrin complexes[7b,12] have been investigated, multivalent (pseudo)rotaxanes have been constructed,[13] and adamantyl–cyclodextrin interactions on surfaces were extensively studied.[12b,14] A recent study by Urbach et al.[15] reported thermodynamic data for di- and trivalent interactions between two peptides, one of which carried
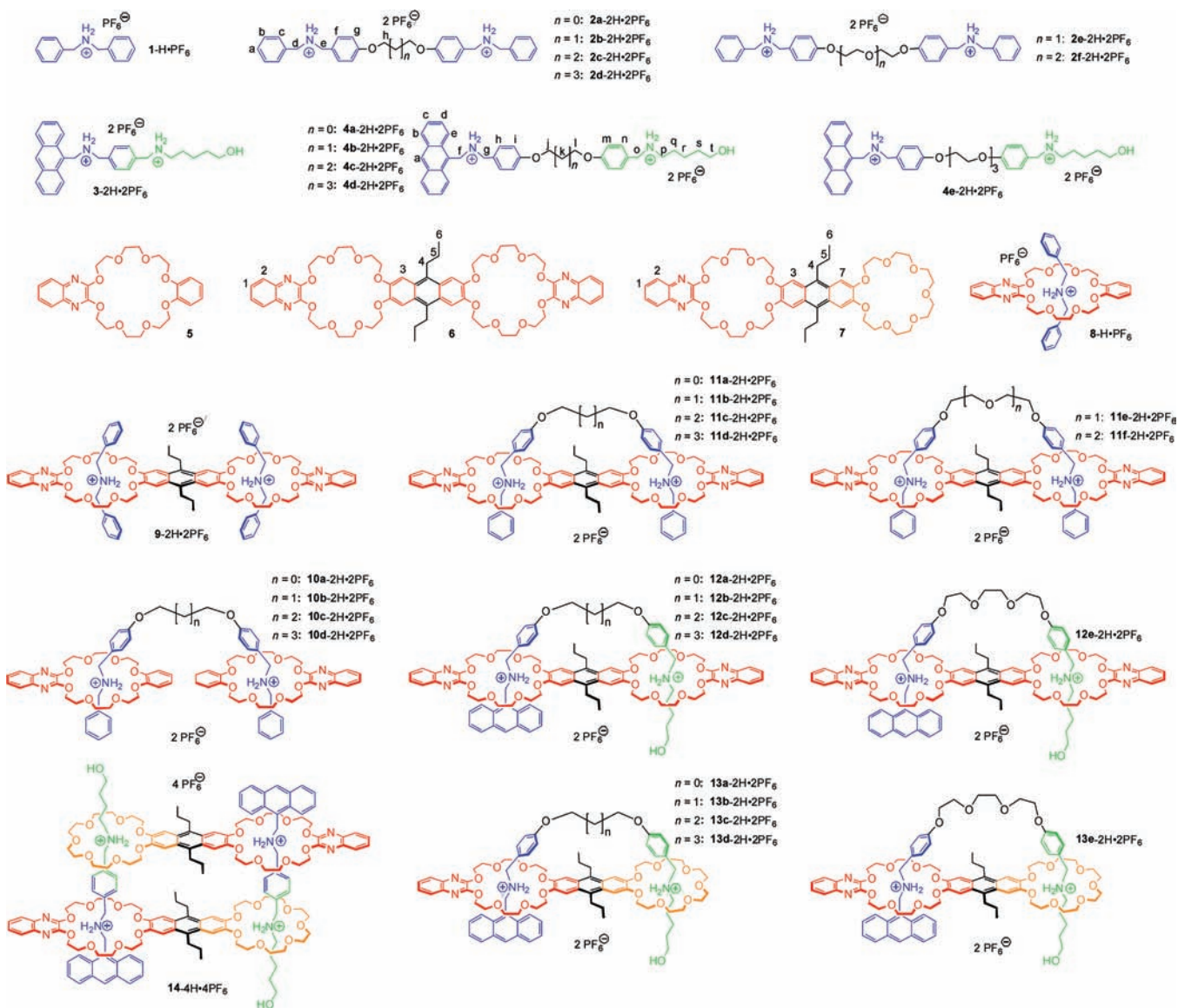
Figure 1. Mono- and divalent axles **1**-H·PF$_6$−**4e**-2H·2PF$_6$, crown ether monomers and dimers **5**−**7**, and pseudorotaxanes **8**-H·PF$_6$−**14**-4H·4PF$_6$ assembled from them. Axle and crown ether protons are labeled with letters and numbers, respectively, to facilitate NMR signal assignment below.

tryptophan side chains, and the other was equipped with methylviologen/cucurbit[8]uril complexes. An up to 280-fold increase in binding constants was observed, but the thermodynamic data revealed the entropic costs of conformational fixation to diminish the total binding energy significantly.

Besides affecting the thermodynamic stability of multivalent complexes, the spacer linking the binding sites can also cause quite substantial kinetic effects. One of Stoddart's trivalent pseudorotaxanes[16] with a rigid spacer exhibited two fast threading steps followed by a third step which took days for completion. Consequently, spacers are not necessarily independent spectators but can alter the binding behavior significantly and may even actively participate in the multivalent binding event.

The present study investigates the chelate cooperativity and spacer-length dependence of the thermodynamic stabilities and assembly kinetics of divalent crown ether/secondary ammonium pseudorotaxanes[17] (Figure 1). Figure 2 illustrates the concept: The thermodynamic (binding constants) and kinetic (guest exchange half-lives) stabilities of three previously reported monovalent pseudorotaxanes are summarized in the center.[10e] Due to the two identical binding sites, *homo*divalent pseudorotaxanes **11a**-2H·2PF$_6$−**11f**-2H·2PF$_6$ facilitate the thermodynamic analysis (Figure 2, left). Using the benzyl ammonium/24-crown-8 motif is advantageous, because it combines sufficiently fast threading−dethreading equilibria for isothermal titration calorimetry (ITC) experiments with a substantial binding energy.[18] Instead, the kinetics of the last threading step can be easily studied in *hetero*divalent pseudorotaxanes **13a**-2H·2PF$_6$−**13e**-2H·2PF$_6$, because the threading of the "green" hydroxypentyl ammonium part through the 21-crown-7 ether is much slower than the preceding threading of the axle through the larger 24-crown-8 moiety.[10e−g] With all building blocks available, the **12a**-2H·2PF$_6$−**12e**-2H·2PF$_6$ pseudorotaxanes serve as the links between the other two series. Monovalent building blocks **1** and **5** are needed to acquire thermodynamic data for **8**-H·PF$_6$, **9**-2H·2PF$_6$, and **10a**-H·PF$_6$−**10d**-H·PF$_6$, without which a detailed analysis of the chelate cooperativity is not possible. Axle **3**-2H·2PF$_6$ is too short to span both crown ethers in **6** or **7** and thus forms quadruply threaded complexes **14**-4H·4PF$_6$. Because only the spacer length changes between four and ten
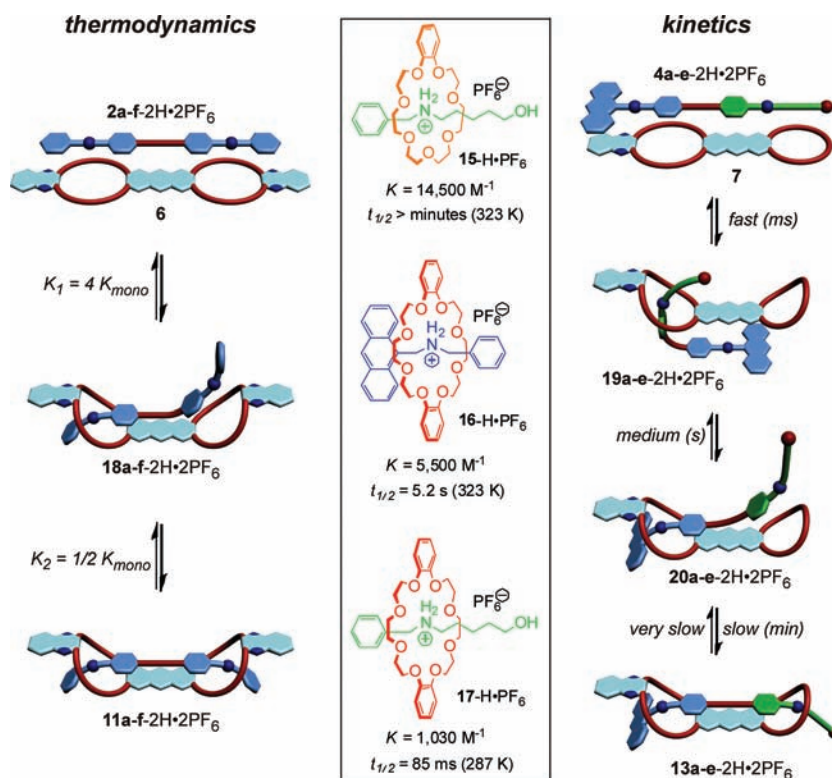
Figure 2. Center: Trends of thermodynamic and kinetic stabilities in three previously reported monovalent monovalent pseudorotaxanes (CD_3Cl : CD_3CN = 2:1).[10e] Because the phenyl group of the "blue" axle is too bulky to thread through the 21-crown-7 ether, no pseudorotaxane forms from the blue axle and 21-crown-7 ethers. Left: Thermodynamic model for divalent binding. Right: Kinetic path selection and the different time scales of the three threading steps permit separate analysis of the final threading event.

atoms connecting the two axle phenyl groups within each series of axles **2a**-2H·PF_6—**2f**-2H·PF_6 and **4a**-2H·PF_6—**4e**-2H·PF_6, the influence of the spacers on the thermodynamic and kinetic properties of the divalent pseudorotaxanes can be directly analyzed.
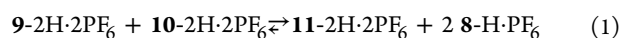
■ RESULTS AND DISCUSSION

Synthesis and Characterization of Axles, Crown Ethers, and Pseudorotaxanes. The syntheses and analytical data of new building blocks and pseudorotaxanes are reported in detail in the Supporting Information. Consequently, we restrict ourselves to a few remarks and the discussion of one homo- and one heterodivalent pseudorotaxane here. The 24-crown-8 homodimer bears quinoxaline groups, which facilitate the dimerization of **5** with two molecules of butanal under strongly acidic conditions (82% H_2SO_4).[10f] If for example dibenzo-24-crown-8 was used, this reaction could occur on both sides and oligomerization would not only reduce the yield but would also render product isolation difficult.[10a] With the quinoxaline, one side is blocked and the dimerization can only occur with the benzo moiety.

The exclusive formation of homo- and heterodivalent pseudorotaxanes **11a**-2H·$2PF_6$—**13e**-2H·$2PF_6$ from the corresponding axles and wheels is supported by typical[10f] complexation-induced shifts in the ^{1}H NMR and by ESI-MS experiments.[10e,19] Signal assignment was performed from the ^{1}H,^{1}H COSY NMR spectra (see Supporting Information). As representative examples, the ^{1}H NMR spectra of **11a**-2H·$2PF_6$ and **13a**-2H·$2PF_6$ (Figures 3b,e) are compared with those of the corresponding axles (Figures 3a,d) and wheels (Figures 3c,f). In the spectra of **11a**-2H·$2PF_6$, substantial signal shifts to higher field are observed for protons *g* ($\Delta\delta$ = 0.78 ppm) and *h* ($\Delta\delta$ = 1.71 ppm). The corresponding

protons in **13a**-2H·$2PF_6$ experience similar signal shifts: *i* and *m* both shift by $\Delta\delta \sim 0.8$ ppm and *j* and *l* by $\Delta\delta \sim 1.7$ ppm. These large upfield shifts can only be explained when these spacer protons are located directly above the anthracene unit connecting the two crown ethers. Upon divalent binding, this is the case, while monovalent binding or the formation of oligomers would not fix these protons above the anthracene. No signals are observed for free axle and crown binding sites so that we conclude the divalent pseudorotaxanes to be the by far dominating species in solution. The other less prominent complexation-induced signal shifts are in good agreement with this interpretation, which also holds for the other pseudorotaxanes under study (Supporting Information). Also, ESI mass spectrometry supports the formation of divalent pseudorotaxanes (Supporting Information). For each pseudorotaxane, clean mass spectra are obtained in which the only significant signal corresponds to the doubly charged pseudorotaxane ions $[\mathbf{11a}\text{-}2H]^{2+}$ (m/z 781) and $[\mathbf{13a}\text{-}2H]^{2+}$ (m/z 757).[19]

Double Mutant Cycles for the Analysis of Chelate Cooperativity. A detailed thermodynamic description of the binding in our divalent pseudorotaxanes requires the analysis of chelate cooperativity, which was examined earlier for other systems by Anderson et al.,[20] Ercolani et al.,[21] Hunter et al.,[22] and others.[2b,12a,23] Here, we use the double mutant cycle concept[22d,g] shown in Figure 4 for the analysis of the (always positive)[21c] chelate cooperativity in the divalent pseudorotaxanes under study. This cycle is derived from the disproportionation equilibria in eq 1.
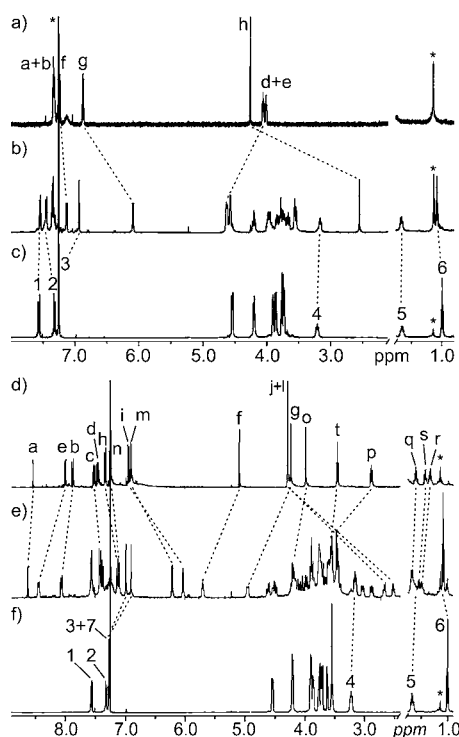
$$\mathbf{9}\text{-}2H·2PF_6 + \mathbf{10}\text{-}2H·2PF_6 \rightleftarrows \mathbf{11}\text{-}2H·2PF_6 + 2\ \mathbf{8}\text{-}H·PF_6 \quad (1)$$

Figure 3. ¹H NMR spectra (500 MHz, 298 K, CDCl₃:CD₃CN = 5:1, 2.0 mM) of (a) axle **2a**-2H·2PF₆, (b) pseudorotaxane **11a**-2H·2PF₆, (c) crown ether homodimer **6**, (d) axle **4a**-2H·2PF₆, (e) pseudorotaxane **13a**-2H·2PF₆, and (f) crown ether heterodimer **7**. Dotted lines indicate complexation-induced signal shifts. Signal assignments are based on ¹H,¹H COSY NMR experiments. Labels refer to those shown in Figure 1. Asterisk = residual solvent. The corresponding ESI mass spectra are shown in the Supporting Information.

If the formation of the divalent pseudorotaxane occurs with strongly positive cooperativity, the equilibrium shifts far to the product side (eq 1). Double mutant cycles eradicate all effects that are not due to chelate cooperativity. For example, connecting two monovalent crown ethers by the anthracene spacer might change the electronic properties of the aromatic system attached to the crowns and thus may have an effect on their

binding strengths. Because two copies of the monovalent and one copy of the divalent crown ethers appear on each side of eq 1, this effect cancels. Similarly, connecting two axle benzyl groups by aryl ethers certainly makes the two aromatic rings more electron-rich and has an effect on their $\pi-\pi$ stacking abilities and their C–H···O hydrogen bonding[24] capabilities. Again, this effect cancels for analogous reasons, like all others that are not due to chelate cooperativity. All binding constants, i.e. K^A, K_1^B, K_2^B (and thus K^B), K_1^C, K_2^C (and with them K^C), K_{mono} and with it K^D, can be determined by assembling the different mono- and divalent components of the pseudorotaxanes in four separate experiments corresponding to those shown in Figure 4A–D.

For the equilibrium in eq 1, the free enthalpy change $\Delta\Delta G$ can be described as the difference of the contributions of the individual complexes involved (eq 2) and the equilibrium constant as in eq 3.

$$\Delta\Delta G = \Delta G^A + \Delta G^D - \Delta G^B - \Delta G^C \qquad (2)$$

$$K = \frac{K^A K^D}{K^B K^C} \qquad (3)$$

Inserting the expressions for K^A to K^D from Figure 4A–D yields the effective molarity EM (eq 4). Thus, from the binding constant accessible by experiments, the effective molarity can be calculated providing a measure to judge the magnitude of chelate cooperativity in the pseudorotaxanes under study.[22c,d]

$$K = \frac{2K_{mono}^2 EM K_{mono}^2}{K_{mono}^2 K_{mono}^2} = 2EM \quad \text{or} \quad EM = \frac{K^A K^D}{2K^B K^C} \qquad (4)$$

Spacer Effects on the Thermodynamic Binding Data from Isothermal Titration Calorimetry (ITC). The thermodynamic binding data for the mono- and divalent pseudorotaxanes under study are summarized in Table 1 as obtained from ITC experiments. It is widely accepted that ITC measurements provide accurate data for systems, in which the so-called Wiseman c value[25] (eq 5) is between 10 and 1000. In this equation, n represents the number of binding sites, K_a the binding constant, and $[H]_{tot}$ the total host concentration. Wiseman
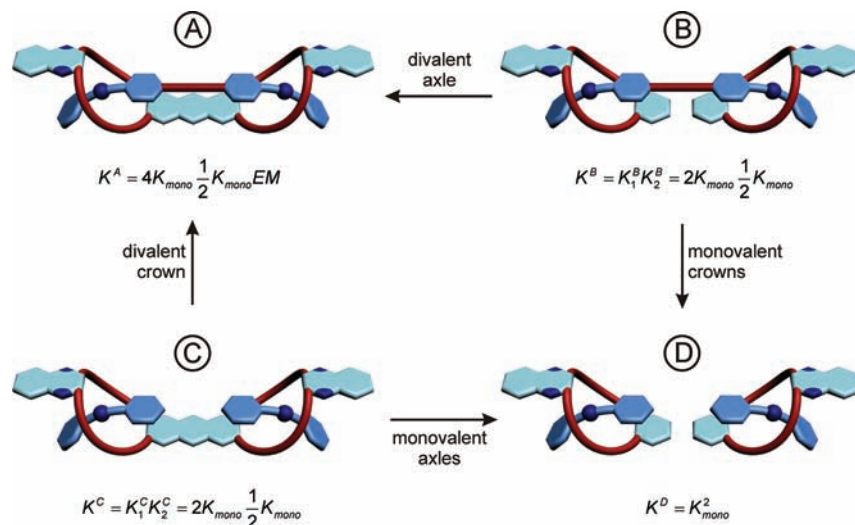

Figure 4. Double mutant cycle for the disproportionation equilibrium in eq 1. Divalent pseudorotaxanes exhibiting strong positive chelate cooperativity shift this equilibrium further (large negative $\Delta\Delta G$ and high EM values) to the product side than that of weakly cooperative systems (small negative $\Delta\Delta G$ and low EM values).

Table 1. Thermodynamic Binding Data As Obtained from ITC Titrations (CHCl$_3$/CH$_3$CN = 2.2:1, 298 K)

		K_a [M^{-1}]	ΔG [kJ mol^{-1}]	ΔH^a [kJ mol^{-1}]	$-T\Delta S^a$ [kJ mol^{-1}]	EM^b [mM]
8-H·PF$_6$		420 ± 50	−15.0 ± 0.3	−61.3	+46.3	
9-2H·2PF$_6$	K_1	735 ± 90	−16.4 ± 0.3	−48.0	+31.7	
	K_2	145 ± 20	−12.3 ± 0.4	−75.2	+62.8	
10a-2H·2PF$_6$	K_1	714 ± 90	−16.3 ± 0.3	+2.9	−19.2	
	K_2	220 ± 30	−13.3 ± 0.4	−3.9	−9.4	
11a-2H·2PF$_6$		25,000 ± 2,500	−25.1 ± 0.3	−71.3	+46.2	132
11b-2H·2PF$_6$		1,100 ± 100	−17.4 ± 0.2	−66.5	+49.1	5.8
11c-2H·2PF$_6$		700 ± 60	−16.2 ± 0.2	−68.9	+52.7	3.7
11d-2H·2PF$_6$		560 ± 50	−15.7 ± 0.2	−69.2	+53.5	3.0
11e-2H·2PF$_6$		630 ± 60	−16.0 ± 0.3	−66.7	+50.7	
11f-2H·2PF$_6$		480 ± 50	−15.3 ± 0.3	−67.2	+51.9	

$^a\Delta H$ and ΔS values have larger errors than those of ΔG and should be regarded as estimates rather than precise values. ^{b}The EM values were calculated using the experimentally determined K^A, K_1^B, K_2^B, K_1^C K_2^C, and $K^D = K_{mono}^2$ values.

c values within this range are often difficult to achieve for low affinity systems, because the low binding constant would require high concentrations for compensation that result in solubility problems. For the pseudorotaxanes discussed here, the c values are in the range of 2 (**11f**-2H·2PF$_6$) to 100 (**11a**-2H·2PF$_6$).

$$c = nK_a[\text{H}]_{tot} \qquad (5)$$

A recent report by Turnbull and Daranas[26] showed, however, that accurate data can also be obtained for small c values. Because the curvatures of our titration curves are well-defined, the binding constants K_a and with them the free enthalpies of binding ΔG can be obtained by curve fitting with errors of about ±10%. Instead, the errors of ΔH and ΔS are likely larger, because the titration curves do not have the typical sigmoidal shape which defines the step size and with it provides a precise value for ΔH. As a control experiment for the accuracy of the ΔG values, we performed ^{1}H NMR competition experiments and offered two different axles to the crown dimer in a 3:3:2 ratio (Supporting Information). The pseudorotaxane axle protons g are not superimposed by any other signal, while their positions differ depending on the spacer length. Consequently, their integrations could easily be evaluated to obtain $\Delta\Delta G$ values for couples of pseudorotaxanes. These experiments result in a trend, which closely parallels the binding energy differences obtained from the ITC experiments. Together with the arguments put forward by Turnbull and Daranas,[27] we therefore conclude that the free binding enthalpies ΔG in Table 1 are sufficiently precise to evaluate the chelate cooperativity of the pseudorotaxanes under study.

The binding constant of $K_{mono} = 420$ M^{-1} for pseudorotaxane **8**-H·PF$_6$ describes the monovalent binding event. The formation of **9**-2H·2PF$_6$ should proceed in two steps. Including statistical factors,[27] the first binding constant K_1 should be twice K_{mono}, and the second one, K_2, a half K_{mono}. The two constants measured for **9**-2H·2PF$_6$ are close to these expected values, as are K_1 and K_2 for **10a**-2H·2PF$_6$. Because the values for these two complexes are very similar, we can, in agreement with a recent literature report,[28] safely assume those of **10b–f**-2H·2PF$_6$ to be in the same ranges. Consequently, the values for **10a**-2H·2PF$_6$ were used for all EM calculations.

The binding constants for the divalent pseudorotaxanes **11a–f**-2H·2PF$_6$ significantly depend on the spacer length with a sharp drop from 25 000 M^{-1} for **11a**-2H·2PF$_6$ (C$_2$-spacer) to 1100 M^{-1} for **11b**-2H·2PF$_6$ (C$_3$-spacer). For even longer spacers, the decrease in K_a is less drastic. With 132 mM, the

effective molarity is particularly high for **11a**-2H·2PF$_6$ and then drastically drops to less than 10 mM for the other divalent pseudorotaxanes. Consequently, chelate cooperativity is particularly pronounced for the pseudorotaxane bearing a C$_2$-spacer between the two axle phenols.

In their essay on cooperativity,[22f] Anderson and Hunter use the dimensionless quantity K_{mono}EM as a measure of cooperativity. If K_{mono}EM $\gg$ 1, the system exhibits positive cooperativity, if K_{mono}EM $\ll$ 1, the system prefers the partially bound state. For **11a**-2H·2PF$_6$, we calculate K_{mono}EM to be 40, clearly indicating a highly positive cooperativity for this system. For longer spacer lengths, the K_{mono}EM values are around 1 to 2 so that the cooperativity of binding is not significantly positive here.

A Rationalization of the Pronounced Chelate Cooperativity of 11a-2H·2PF$_6$ Based on its Crystal Structure.[29] The addition of a single methylene group drastically decreases the effective molarity between **11a**-2H·2PF$_6$ and **11b**-2H·2PF$_6$. Because only the spacer is varied, the question arises: why such a significant change in cooperativity? This finding clearly points to noninnocent spacers, which contribute to the overall free binding enthalpies. A view of the crystal structure of **11a**-2H·2PF$_6$ (Figure 5) provides further insight. Not unexpectedly,[30] the binding between the axle ammonium groups and the crown ethers are mediated by two moderate N−H···O hydrogen bonds at each ammonium cation[31] and weak C−H···O hydrogen bonds involving the polarized methylene groups next to the ammonium cations.[32] The C2 spacer in the axle center almost exactly spans the two axle phenols placing them directly above the anthracene spacer between the two crown ethers. The plane-to-plane distances[33] nicely match that expected for π-stacked complexes. Consequently, a complex forms in which the two axle phenols are perfectly preorganized for $\pi-\pi$ stacking interactions with the anthracene. The addition of one or more methylene groups in the axle center necessarily induces deviations of the two phenols from this close-to-perfect arrangement. In view of the double mutant cycle shown above, it should be noted that the preorganizing effect of the C$_2$ spacer modulates the $\pi-\pi$ interactions. It is this modulation, not the absolute $\pi-\pi$ stacking interaction, which causes the pronounced chelate cooperativity. The longer spacers cannot arrange the two phenols in such a nearly perfect geometry. Consequently, the modulation of the $\pi-\pi$ interactions decreases and no such pronounced cooperativity effect is observed for these pseudorotaxanes.

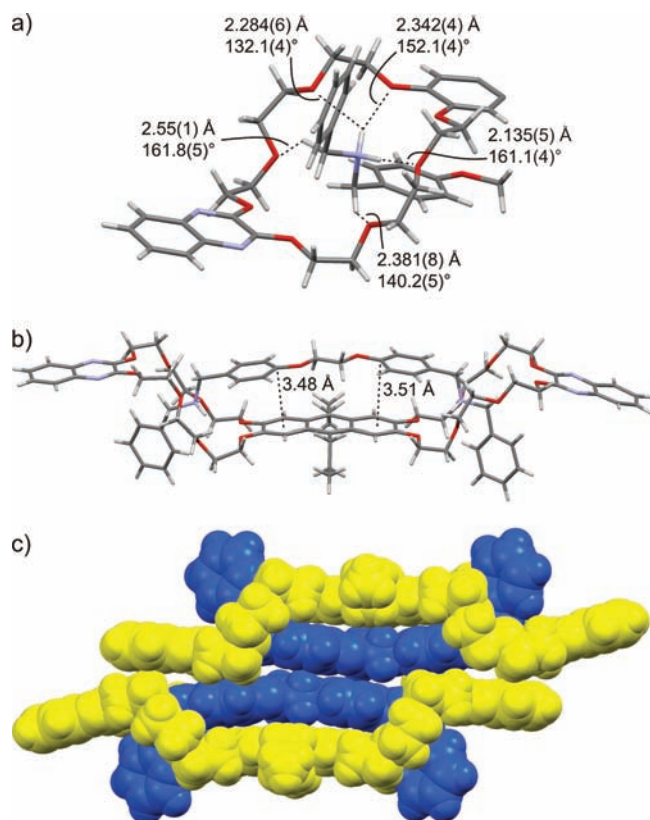**Kinetics: Heterodivalent Pseudorotaxanes.** The divalent pseudorotaxanes above form through two threading steps.

Figure 5. Crystal structure of pseudorotaxane 11a-2H·2PF₆. (a) Cut-out of one crown-axle binding motif: N—H···O and C—H···O hydrogen bonds connecting the crown and the axle on one side of the divalent pseudorotaxane. Note that the exact lengths and angles are somewhat different for the second binding site (see text). (b) The whole complex and plane-to-plane distances between axle phenyl rings and the anthracene spacer of the crown ether dimer. (c) Space filling representation and view of the packing of two neighboring complexes (axle: blue, crown dimer: yellow). For more crystallographic details, see Supporting Information.

The kinetics of the first one should be more or less spacer-independent, while the second threading event can be expected to be affected by the spacer between the two ammonium ions. To be able to compare the thermodynamic spacer effects with the kinetic ones, it would thus be preferable if the second, spacer-dependent threading step could be monitored independently. For this reason, the heterodivalent pseudorotaxanes 13a−e-2H·2PF₆ (Figure 1) were chosen, because they bear orthogonal and thus clearly distinguishable binding sites.[10e−g] The anthracene stopper of axles 4a−e-2H·2PF₆ ensures sequential threading to exclusively occur from one side of the axle. As a consequence, threading now involves three steps (Figure 2): (i) A fast threading of the 24-crown-8 moiety onto the hydroxypentyl ammonium site occurs on a millisecond time scale[10e] and yields 19a−e-2H·2PF₆. This step happens more or less exclusively, because the slipping of the smaller 21-crown-7 ether onto the axle is much slower. (ii) Migration of the 24-crown-8 ether to the second, anthracenyl methyl ammonium station proceeds on a second time scale[10e] and gives rise to 20a−e-2H·2PF₆. (iii) Finally, threading of the smaller 21-crown-7 ether onto the hydroxypentyl ammonium group requires many minutes[10e] and completes the formation of the pseudorotaxanes 13a−e-2H·2PF₆. Consequently, intermediates 20a−e-2H·2PF₆ accumulate before the last step occurs. Their conversion to the final pseudorotaxane can thus be monitored

by ¹H NMR spectroscopy. To prepare the kinetics study, the following two experiments were performed:

(i) To make sure that the thermodynamic trends remain unaltered with the unsymmetrical axles 4a−e-2H·PF₆, ¹H NMR competition experiments like those discussed above were performed with pseudorotaxanes 12a−e-2H·2PF₆ and 13a−e-2H·2PF₆ (see Supporting Information). The same trends were obtained so that we conclude the transition from axles 2a−e-2H·PF₆ to 4a−e-2H·PF₆ to likely alter the absolute, but not the relative, spacer-induced stabilities.

(ii) Figure 6 shows the temporal development of a 1:1:1 mixture of axles 4a-2H·PF₆ and 4b-2H·PF₆ with crown heterodimer 7.
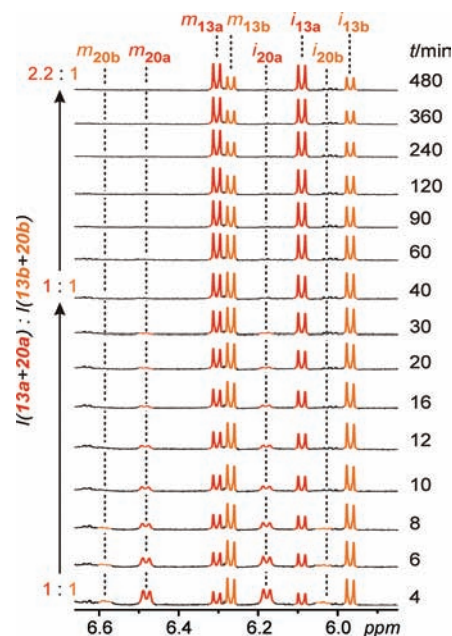

Figure 6. Temporal development of a 1:1:1 mixture of 4a-2H·2PF₆, 4b-2H·2PF₆, and 7 (500 MHz, 298 K, CDCl₃:CD₃CN = 2:1, 5.0 mM). Reaction intervals are given on the right side, the evolution of integral ratios on the left. m and i denote the axle protons ortho to the phenol O atoms (Figure 1).

Protons i and m ortho to the phenol oxygen atoms are most indicative of the formation of intermediates 20a-2H·PF₆ and 20b-2H·PF₆ and the final divalent pseudorotaxanes 13a-2H·PF₆ and 13b-2H·PF₆. From this experiment, four conclusions can be drawn: First, the signals are all separate from each other so that it is possible to follow the kinetics of pseudorotaxane formation quantitatively. Second, intermediate 20b-2H·PF₆ is converted more quickly to 13b-2H·PF₆ than 20a-2H·PF₆ to 13a-2H·PF₆. Consequently, the shorter C₂ spacer does not foster the highest threading rate. Rather, the C₃ spacer reacts through the lower activation barrier. Although 20b-2H·PF₆ vanishes within the first few minutes at room temperature, it will still be possible to quantitatively follow the kinetics at lower temperatures. The third conclusion is derived from the integrals: When the sum of the integrals of 13a-2H·PF₆ and 20a-2H·PF₆ is compared to the sum of 13b-2H·PF₆ and 20b-2H·PF₆, the ratio is 1:1 and remains constant for about the first 40 min. At about that time, the intermediates 20a-2H·PF₆ and 20b-2H·PF₆ have been fully converted into the heterodivalent pseudorotaxane products. A very slow error correction then leads to a decrease of 13b-2H·PF₆ relative to 13a-2H·PF₆ in line with the thermodynamics discussed above for the homodivalent pseudorotaxanes.

The constant 1:1 integral ratio observed at the beginning of the experiment clearly indicates that the first two threading steps giving rise to intermediates **20a,b**-2H·PF$_6$ do not depend on the spacer, while the third threading event does (Figure 2, right). The stabilities of the intermediates are independent of the length of the spacers, and statistically a half of host **7** will be consumed by **4a**-2H·2PF$_6$ and a half by **4b**-2H·2PF$_6$. Consequently, it is possible to investigate the kinetics of the final step independently from the preceding ones, and the model depicted in Figure 2 (right) fits the experiments. Finally, the back-reaction from intermediates **20a,b**-2H·PF$_6$ to the reactants is significantly slower than the forward reaction to the final pseudorotaxanes. Otherwise, the spectrum obtained after 40 min would not show a 1:1 ratio of the two pseudorotaxanes. In addition, the dethreading of the green axle from 21-crown-7 is also very slow compared to the forward threading step. Error-correction, which starts to become visible after ca. 40 min, leads to the thermodynamically predominant stable complex **13a**-2H·PF$_6$ shown in Figure 6. This is important, because the last threading step can then be treated with a simple quasi-irreversible unimolecular kinetic model (eq 6). The activation parameters are accessible by determining the rate constants at different temperatures with the help of the Eyring equation (eq 7).

$$\ln\left(\frac{c}{c_0}\right) = -kt \tag{6}$$

$$\ln\frac{k}{T} = -\frac{\Delta H^{\ddagger}}{R}\frac{1}{T} + \frac{\Delta S^{\ddagger}}{R} + \ln\frac{k_B}{h} \tag{7}$$

Spacer Effects on the Activation Parameters of the Final Threading Step. The rate constants for the final threading step have been measured at different temperatures for all five pseudorotaxanes **13a–e**-2H·2PF$_6$ (Supporting Information). The activation parameters are summarized in Table 2.

Table 2. Activation Parameters for the Final Intramolecular Threading Step Converting 20a–e-2H·2PF$_6$ into 13a–e-2H·2PF$_6$ (determined on a 500 MHz NMR spectrometer (CDCl$_3$:CD$_3$CN = 2:1, 5.0 mM)

	$\Delta G^{\ddagger}$ (298 K) [kJ mol^{-1}]	$\Delta H^{\ddagger}$ [kJ mol^{-1}]	$-T\Delta S^{\ddagger}$ (298 K) [kJ mol^{-1}]
13a-2H·PF$_6$	91.9 ± 2.0	59.2 ± 1.8	32.7 ± 1.9
13b-2H·PF$_6$	86.7 ± 1.8	53.3 ± 1.6	33.4 ± 1.8
13c-2H·PF$_6$	84.7 ± 2.3	49.7 ± 2.3	35.0 ± 2.7
13d-2H·PF$_6$	84.2 ± 1.1	49.0 ± 0.9	35.2 ± 1.0
13e-2H·PF$_6$	85.2 ± 2.5	47.5 ± 2.3	37.7 ± 2.7

The free enthalpies of activation decrease with spacer length from ca. 92 kJ mol^{-1} for the C$_2$-spacer in **13a**-2H·2PF$_6$ to ca. 84 kJ mol^{-1} for the C$_5$-spacer in **13d**-2H·2PF$_6$ and then slightly increases again (though within experimental error) for **13e**-2H·2PF$_6$. Consequently, the spacer giving rise to the maximum binding strengths exhibits the highest activation barrier.

A closer look at the activation enthalpies and entropies points to the reasons for this behavior. The activation enthalpy for the formation of **13a**-2H·2PF$_6$ is particularly high, indicating the presence of some strain in the transition state. With longer spacers, the strain is released and the activation enthalpy decreases. All activation entropies are negative as expected for a situation in which a freely mobile chain is fixed through intramolecular ring formation. The longer the spacer, the larger this

effect becomes. Entropically, the C$_2$-spacer is thus favorable due to the lower number of degrees of freedom that are fixed upon the last threading effect. At chain lengths around C$_5$, the third threading event is not governed by strain (enthalpy) anymore and the entropic effects originating from conformational fixation take over. This leads to a slight increase of the activation barrier for longer spacers. Kinetically, the fastest threading thus occurs around this spacer length , and thus the kinetically optimum spacer length clearly differs from the thermodynamic one.

CONCLUSIONS

The following conclusions can be drawn from the results discussed above:

(i) Already quite subtle changes in the spacer length such as the introduction of an additional methylene group in an alkyl chain can cause substantial alterations in multivalent binding. A model that describes multivalent binding by just considering the binding sites as connected through an innocent, flexible molecular thread can be too simple for an accurate description when dealing with short spacers. In the C$_2$-spacer pseudorotaxane **11a**-2H·2PF$_6$, the spacer participates in binding through a significant preorganization effect which increases the binding strength and with it causes strong positive chelate cooperativity.

(ii) Multivalency can be expressed thermochemically, i.e., in binding constant variations, but it can also be expressed kinetically. No direct correlation between the thermodynamics and kinetics need to exist. In the examples discussed here, the spacer optimal for strong binding is unfavorable for the final threading step, because it induces strain in the transition structure, which does not exist anymore in the final product.

(iii) In view of the analysis of spacer length in the article by Kramer and Karpen[4] mentioned in the Introduction, similar trends are found here: A too short spacer such as the phenyl group in axle **3**-2H·2PF$_6$ can only undergo monovalent binding with one host molecule. Consequently, the remaining binding sites also bind, but the system forms larger assemblies such as **14**-4H·4PF$_6$ to maximize the binding energy.[10e,f] When the spacer becomes long enough to span both binding sites of the host, divalent binding occurs through transition states that are strained and thus enthalpically disfavored with stoppers of intermediate length. Axles with even longer spacers then react more quickly until the entropic penalty for conformational fixation dictates higher barriers again.

(iv) In line with the analysis of entropy effects by Whitesides et al.,[6] the entropic effects of longer spacers are not very pronounced so that significantly overlong, but flexible, spacers still remain potent. With our study, we have shown that similar trends govern divalent binding in both small synthetic supramolecular systems and biological systems.

ASSOCIATED CONTENT

⊙ Supporting Information

Synthetic procedures and characterization data for new compounds; analytical data for pseudorotaxanes including 1D NMR, ^{1}H,^{1}H COSY NMR, and ESI-FTICR mass spectra; experimental details for ^{1}H NMR competition experiments, ITC titrations, and crystal structure determination; rate-constant determination and Eyring plots. This material is available free of charge via the Internet at http://pubs.acs.org.

AUTHOR INFORMATION

Corresponding Author
christoph@schalley-lab.de
Present Address
§The Skaggs Institute for Chemical Biology, The Scripps Research Institute, 10550 N. Torrey Pines Rd., La Jolla, CA 92037.

ACKNOWLEDGMENTS

REFERENCES

(1) (a) Mammen, M.; Choi, S. K.; Whitesides, G. M. *Angew. Chem., Int. Ed.* **1998**, *37*, 2754−2794. (b) Choi, S.-K. *Synthetic Multivalent Molecules*; Wiley: Hoboken, 2004.

(2) (a) Kitov, P. I.; Sadowska, J. M.; Mulvey, G.; Armstrong, G. D.; Ling, H.; Pannu, N. S.; Read, R. J.; Bundle, D. R. *Nature* **2000**, *403*, 669−672. (b) Kitov, P. I.; Bundle, D. R. *J. Am. Chem. Soc.* **2003**, *125*, 16271−16284.

(3) (a) Hartmann, M.; Lindhorst, T. K. *Eur. J. Org. Chem.* **2011**, *2011*, 3583−3609. (b) Schwefel, D.; Maierhofer, C.; Beck, J. G.; Seeberger, S.; Diederichs, K.; Möller, H. M.; Welte, W.; Wittmann, V. *J. Am. Chem. Soc.* **2010**, *132*, 8704−8719. (c) Cairo, C. W.; Gestwicki, J. E.; Kanai, M.; Kiessling, L. L. *J. Am. Chem. Soc.* **2002**, *124*, 1615−1619.

(4) Kramer, R. H.; Karpen, J. W. *Nature* **1998**, *395*, 710−713.

(5) Diestler, D. J.; Knapp, E. W. *J. Phys. Chem. C* **2009**, *114*, 5287−5304.

(6) Krishnamurthy, V. M.; Semetey, V.; Bracher, P. J.; Shen, N.; Whitesides, G. M. *J. Am. Chem. Soc.* **2007**, *129*, 1312−1320.

(7) (a) Badjić, J. D.; Nelson, A.; Cantrill, S. J.; Turnbull, W. B.; Stoddart, J. F. *Acc. Chem. Res.* **2005**, *38*, 723−732. (b) Mulder, A.; Huskens, J.; Reinhoudt, D. N. *Org. Biomol. Chem.* **2004**, *2*, 3409−3424. (c) Röckendorf, N.; Lindhorst, T. K. *Top. Curr. Chem.* **2001**, *217*, 201−238.

(8) (a) Gerbeleu, N. V.; Arion, V. B.; Burgess, J. *Template Synthesis of Macrocyclic Compounds*; Wiley-VCH: Weinheim, Germany, 1999. (b) Diederich, F.; Stang, P. J., Eds. *Templated Organic Synthesis*; Wiley-VCH: Weinheim, Germany, 2000. (c) Busch, D. H.; Stephensen, N. A. *Coord. Chem. Rev.* **1990**, *100*, 119−154.

(9) (a) Lindsey, J. S. *New J. Chem.* **1991**, *15*, 153−180. (b) Philp, D.; Stoddart, J. F. *Angew. Chem., Int. Ed.* **1996**, *35*, 1155−1196. (c) Schalley, C. A.; Lützen, A.; Albrecht, M. *Chem.—Eur. J.* **2004**, *10*, 1072−1080. (d) Whitesides, G. M.; Mathias, J. P.; Seto, C. T. *Science* **1991**, *254*, 1312−1319.

(10) (a) Jiang, W.; Sattler, D.; Rissanen, K.; Schalley, C. A. *Org. Lett.* **2011**, *13*, 4502−4505. (b) Jiang, W.; Wang, Q.; Linder, I.; Klautzsch, F.; Schalley, C. A. *Chem.—Eur. J.* **2011**, *17*, 2344−2348. (c) Brusilowskij, B.; Dzyuba, E. V.; Troff, R. W.; Schalley, C. A. *Chem. Commun.* **2011**, *47*, 1830−1832. (d) Ghosh, S.; Wu, A.; Fettinger, J. C.; Zavalij, P. Y.; Isaacs, L. *J. Org. Chem.* **2008**, *73*, 5915−5925. (e) Jiang, W.; Schäfer, A.; Mohr, P. C.; Schalley, C. A. *J. Am. Chem. Soc.* **2010**, *132*, 2309−2320. (f) Jiang, W.; Schalley, C. A. *Proc. Natl. Acad. Sci. U.S.A.* **2009**, *106*, 10425−10429. (g) Jiang, W.; Winkler, H. D. F.; Schalley, C. A. *J. Am. Chem. Soc.* **2008**, *130*, 13852−13853. (h) Mahata, K.; Saha, M. L.; Schmittel, M. *J. Am. Chem. Soc.* **2010**, *132*, 15933−15935. (i) Mahata, K.; Schmittel, M.

J. Am. Chem. Soc. **2009**, *131*, 16544−16554. (j) Mukhopadhyay, P.; Wu, A.; Isaacs, L. *J. Org. Chem.* **2004**, *69*, 6157−6164. (k) Rudzevich, Y.; Rudzevich, V.; Klautzsch, F.; Schalley, C. A.; Böhmer, V. *Angew. Chem., Int. Ed.* **2009**, *48*, 3867−3871. (l) Schmittel, M.; Mahata, K. *Chem. Commun.* **2010**, *46*, 4163−4165. (m) Tomimasu, N.; Kanaya, A.; Takashima, Y.; Yamaguchi, H.; Harada, A. *J. Am. Chem. Soc.* **2009**, *131*, 12339−12343. (n) Wu, A.; Isaacs, L. *J. Am. Chem. Soc.* **2003**, *125*, 4831−4835. (o) Jiang, W.; Schalley, C. A. *Beilstein J. Org. Chem.* **2010**, *6*, no. 14. (p) Wang, F.; Han, C.; He, C.; Zhou, Q.; Zhang, J.; Wang, C.; Li, N.; Huang, F. *J. Am. Chem. Soc.* **2008**, *130*, 11254−11255.

(11) (a) Casnati, A.; Sansone, F.; Ungaro, R. *Acc. Chem. Res.* **2003**, *36*, 246−254. (b) Sansone, F.; Baldini, L.; Casnati, A.; Ungaro, R. *New J. Chem.* **2010**, *34*, 2715−2728. (c) Wang, L.; Vysotsky, M. O.; Bogdan, A.; Bolte, M; Böhmer, V. *Science* **2004**, *304*, 1312−1314.

(12) (a) Huskens, J. *Curr. Opin. Chem. Biol.* **2006**, *10*, 537−543. (b) Nijhuis, C. A.; Yu, F.; Knoll, W.; Huskens, J.; Reinhoudt, D. N. *Langmuir* **2005**, *21*, 7866−7876. (c) Liu, Y.; Chen, Y. *Acc. Chem. Res.* **2006**, *39*, 681−691.

(13) (a) Badjić, J. D.; Balzani, V.; Credi, A.; Lowe, J. N.; Silvi, S.; Stoddart, J. F. *Chem.—Eur. J.* **2004**, *10*, 1926−1935. (b) Badjić, J. D.; Balzani, V.; Credi, A.; Silvi, S.; Stoddart, J. F. *Science* **2004**, *303*, 1845−1849. (c) Badjić, J. D.; Ronconi, C. M.; Stoddart, J. F.; Balzani, V.; Silvi, S.; Credi, A. *J. Am. Chem. Soc.* **2006**, *128*, 1489−1499.

(14) (a) Huskens, J.; Deij, M. A.; Reinhoudt, D. N. *Angew. Chem., Int. Ed.* **2002**, *41*, 4467−4471. (b) Ludden, M. J. W.; Reinhoudt, D. N.; Huskens, J. *Chem. Soc. Rev.* **2006**, *35*, 1122−1134.

(15) Reczek, J. J.; Kennedy, A. A.; Halbert, B. T.; Urbach, A. R. *J. Am. Chem. Soc.* **2009**, *131*, 2408−2415.

(16) Badjić, J. D.; Cantrill, S. J.; Stoddart, J. F. *J. Am. Chem. Soc.* **2004**, *126*, 2288−2289.

(17) (a) Jiang, W.; Han, M.; Zhang, H.-Y.; Zhang, Z.-J.; Liu, Y. *Chem.—Eur. J.* **2009**, *15*, 9938−9945. (b) Clifford, T.; Abushamleh, A.; Busch, D. H. *Proc. Natl. Acad. Sci. U.S.A.* **2002**, *99*, 4830−4836. (c) Gibson, H. W.; Yamaguchi, N.; Hamilton, L.; Jones, J. W. *J. Am. Chem. Soc.* **2002**, *124*, 4653−4665. (d) Gibson, H. W.; Yamaguchi, N.; Jones, J. W. *J. Am. Chem. Soc.* **2003**, *125*, 3522−3533. (e) Yamaguchi, N.; Gibson, H. W. *Angew. Chem., Int. Ed.* **1999**, *38*, 143−147. (f) Yamaguchi, N.; Gibson, H. W. *Chem. Commun.* **1999**, 789−790. (g) Yamaguchi, N.; Hamilton, L. M.; Gibson, H. W. *Angew. Chem., Int. Ed.* **1998**, *37*, 3275−3279. (h) Zhang, C.; Zhu, K.; Li, S.; Zhang, J.; Wang, F.; Liu, M.; Li, N.; Huang, F. *Tetrahedron Lett.* **2008**, *49*, 6917−6920. (i) Zhu, K.; Zhang, M.; Wang, F.; Li, N.; Li, S.; Huang, F. *New J. Chem.* **2008**, *32*, 1827−1830. (j) Ashton, P. R.; Fyfe, M. C. T.; Martinez-Diaz, M. V.; Menzer, S.; Schiavo, C.; Stoddart, J. F.; White, A. J. P.; Williams, D. J. *Chem.—Eur. J.* **1998**, *4*, 1523−1534. (k) Ashton, P. R.; Fyfe, M. C. T.; Glink, P. T.; Menzer, S.; Stoddart, J. F.; White, A. J. P.; Williams, D. J. *J. Am. Chem. Soc.* **1997**, *119*, 12514−12524. (l) Ashton, P. R.; Chrystal, E. J. T.; Glink, P. T.; Menzer, S.; Schiavo, C.; Spencer, N.; Stoddart, J. F.; Tasker, P. A.; White, A. J. P.; Williams, D. J. *Chem.—Eur. J.* **1996**, *2*, 709−728. (m) Ashton, P. R.; Ballardini, R.; Balzani, V.; Gómez-López, M.; Lawrence, S. E.; Martinez-Díaz, M. V.; Montalti, M.; Piersanti, A.; Prodi, L.; Stoddart, J. F.; Williams, D. J. *J. Am. Chem. Soc.* **1997**, *119*, 10641−10651. (n) Ashton, P. R.; Baldoni, V.; Balzani, V.; Credi, A.; Hoffmann, H. D. A.; Martinez-Diaz, M. V.; Raymo, F. M.; Stoddart, J. F.; Venturi, M. *Chem.—Eur. J.* **2001**, *7*, 3482−3493. (o) Ashton, P. R.; Baxter, I.; Cantrill, S. J.; Fyfe, M. C. T.; Glink, P. T.; Stoddart, J. F.; White, A. J. P.; Williams, D. J. *Angew. Chem., Int. Ed.* **1998**, *37*, 1294−1297.

(18) Liu, Y.; Li, C.-J.; Zhang, H.-Y.; Wang, L.-H.; Li, X.-Y. *Eur. J. Org. Chem.* **2007**, 4510−4516.

(19) Jiang, W.; Schalley, C. A. *J. Mass Spectrom.* **2010**, *45*, 788−798.

(20) (a) Taylor, P. N.; Anderson, H. L. *J. Am. Chem. Soc.* **1999**, *121*, 11538−11545. (b) Sprafke, J. K.; Odell, B.; Claridge, T. D. W.; Anderson, H. L. *Angew. Chem., Int. Ed.* **2011**, *50*, 5572−5575. (c) Gasparini, G.; Bettin, F.; Scrimin, P.; Prins, L. J. *Angew. Chem., Int. Ed.* **2009**, *48*, 4546−4550.

(21) (a) Ercolani, G. *J. Am. Chem. Soc.* **2003**, *125*, 16097−16103. (b) Ercolani, G. *J. Phys. Chem. B* **2003**, *107*, 5052−5057. (c) Ercolani, G.; Schiaffino, L. *Angew. Chem., Int. Ed.* **2011**, *50*, 1762−1768.

(22) (a) Chi, X.; Guerin, A. J.; Haycock, R. A.; Hunter, C. A.; Sarson, L. D. *J. Chem. Soc., Chem. Commun.* **1995**, 2563−2565. (b) Gasparini, G.; Vitorge, B.; Scrimin, P.; Jeannerat, D.; Prins, L. J. *Chem. Commun.* **2008**, 3034−3036. (c) Camara-Campos, A.; Musumeci, D.; Hunter, C. A.; Turega, S. *J. Am. Chem. Soc.* **2009**, *131*, 18518−18524. (d) Hunter, C. A.; Misuraca, M. C.; Turega, S. M. *J. Am. Chem. Soc.* **2011**, *133*, 582−594. (e) Bisson, A. P.; Hunter, C. A. *Chem. Commun.* **1996**, 1723−1724. (f) Hunter, C. A.; Anderson, H. L. *Angew. Chem., Int. Ed.* **2009**, *48*, 7488−7499. (g) Hunter, C. A.; Ihekwaba, N.; Misuraca, M. C.; Segarra-Maset, M. D.; Turega, S. M. *Chem. Commun.* **2009**, 3964−3966.

(23) Huskens, J.; Mulder, A.; Auletta, T.; Nijhuis, C. A.; Ludden, M. J. W.; Reinhoudt, D. N. *J. Am. Chem. Soc.* **2004**, *126*, 6784−6797.

(24) (a) Castellano, R. K. *Curr. Org. Chem.* **2004**, *8*, 845−865. (b) Ashton, P. R.; Fyfe, M. C. T.; Hickingbottom, S. K.; Stoddart, J. F.; White, A. J. P.; Williams, D. J. *J. Chem. Soc., Perkin Trans 2* **1998**, 2117−2128.

(25) (a) Fisher, H. F.; Singh, N. *Methods Enzymol.* **1995**, *259*, 194−221. (b) Indyk, L.; Fisher, H. F. *Methods Enzymol.* **1998**, *295*, 350−364.

(26) Turnbull, W. B.; Daranas, A. H. *J. Am. Chem. Soc.* **2003**, *125*, 14859−14866.

(27) Ercolani, G.; Piguet, C.; Borkovec, M.; Hamacek, J. *J. Phys. Chem. B* **2007**, *111*, 12195−12203.

(28) Misuraca, M. C.; Grecu, T.; Freixa, Z.; Garavini, V.; Hunter, C. A.; van Leeuwen, P. W. N. M.; Segarra-Maset, M. D.; Turega, S. M. *J. Org. Chem.* **2011**, *76*, 2723−2732.

(29) For the crystallographic details, see the Supporting Information. The structural data have been deposited at the Cambridge Crystallographic Data Center under CCDC no. 853183.

(30) Raymo, F. M.; Bartberger, M. D.; Houk, K. N.; Stoddart, J. F. *J. Am. Chem. Soc.* **2001**, *123*, 9264−9267.

(31) N-H⋯O hydrogen bond parameters: 2.14 Å (H78b⋯O10), 2.28 Å (H78a⋯O15) and 161.1° (N78−H78b−O10), 132.1° (N78−H78a−O15) and 2.02 Å (H97a⋯O7), 2.61 Å (H97b⋯O2) and 170.7° (N97−H97a−O7), 128.2° (N97−H97b−O2).

(32) C-H⋯O hydrogen bond parameters: 2.38 Å (H79a⋯O11), 2.55 Å (H77a⋯O14), and 2.59 Å (H77b⋯O11) and 140.2° (C77−H79a−O11), 161.8° (C77−H77a−O14) and 135.6° (C77−H77b−O11) and 2.38 Å (H96b⋯O3) and 155.9° (C96−H96a−O3).

(33) The normal from C90 to the plane through C2−C7 = 3.51 Å and the normal from C83 to the plane of C9−C14 = 3.48 Å.